X-ray measurement of chain orientation in non-crystalline polymers

Martin Pick*, Richard Lovell and Alan H. Windle
Department of Metallurgy & Materials Science, University of Cambridge, Pembroke Street, Cambridge CB2 3QZ, UK
(Received 3 March 1980)

A new method of orientation measurement using wide angle X-ray scattering (WAXS) is described and compared with methods based on birefringence and spectroscopy. It is applied to PMMA deformed in the glassy or rubbery states. For specimens plastically deformed in uniaxial tension, a comparison is made between orientation parameters measured from WAXS and similar parameters obtained from the same specimens using n.m.r. by Ward. The WAXS method is further used to measure orientation in material deformed in plane-strain compression. It also demonstrates the absence of chain alignment in elastically strained PMMA despite the high birefringence observed.

INTRODUCTION

The orientation of the molecular chains is the most important variable property of any non-crystalline polymer. It is largely controlled by processing history, and has a marked influence on the mechanical properties of the material. It is not surprising that a wide range of physical techniques have been developed to measure chain orientation[1-5]. As part of a wider study of structural aspects of non-crystalline polymers using wide angle X-ray scattering (WAXS), we have applied this technique to the measurement of orientation. The method developed has important advantages over those already established but it also has some particular limitations. However, the assumptions underlying some of the other techniques of measuring orientation are not always appreciated and we first discuss some of these.

The most commonly used method for non-crystalline polymers is to measure the birefrengence of the oriented but unstressed material which, for uniaxial symmetry, is given by[1]

$$\Delta n = \Delta n_{max} f$$

where $\Delta n = n_z - n_x = (n_z - n_y)$ and n_i is the refractive index in the ith direction.

$$f = \langle P_2(\cos\alpha)\rangle = \frac{1}{2}(3\langle\cos^2\alpha\rangle - 1)$$

is the Hermans orientation parameter, P_2 is the 2nd order Legendre polynomial, α is the angle between the axis of the chain segment and the z-axis of the specimen, and Δn_{max} is the birefringence that would be measured for a perfectly aligned specimen. The average $\langle\ \rangle$ is calculated over all segments i.e.

$$\langle\cos^2\alpha\rangle = 2\pi\int_0^{\pi/2} D(\alpha)\cos^2\alpha\sin\alpha\,d\alpha$$

where $D(\alpha)$ is the orientation distribution function and

$$2\pi\int_0^{\pi/2} D(\alpha)\sin\alpha\,d\alpha = 1$$

Hence the orientation parameter f is given by

$$f = \frac{\Delta n}{\Delta n_{max}}$$

which is zero for random orientation and unity for perfect orientation parallel to the specimen axis. Since perfect orientation cannot be achieved, the value of Δn_{max} must be derived either from measurements of optical anisotropy in solution or in the rubber (assuming the conformation is the same), or from calculations of segmental anisotropy (assuming a particular conformation for the chain segments). The difficulties of deriving absolute values of f from birefringence data have been discussed by Stein and Read[1].

A number of spectroscopic methods can also be used to measure orientation in both crystalline and non-crystalline polymers[3]. Infrared dichroism is usually only applicable to thin films and, moreover, needs conformational evidence to assign the angle that the transition moment vector makes with the segment axis[2]. While polarized Raman scattering can be used with thick specimens, there is still the problem of assigning an orientation for the Raman tensor with respect to the segment axis[4].

Broadline nuclear magnetic resonance (n.m.r.) can also be used on thick specimens but has the disadvantage of needing a complete specification of the molecular

* Present Address: ICI Fibres, Hookstone Road, Harrogate, North Yorkshire

0032-3861/80/091017-08$02.00

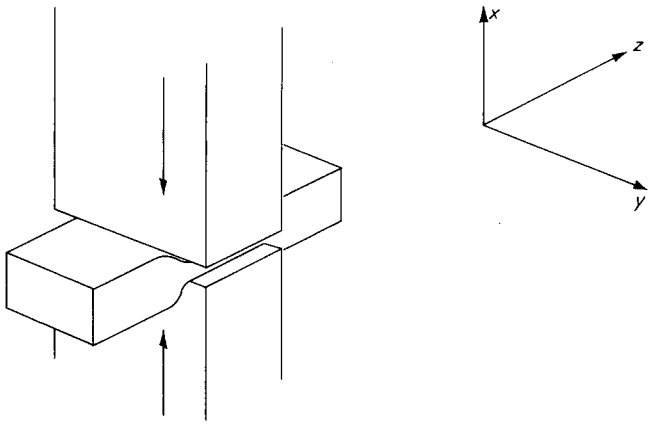

Figure 1 Schematic diagram of plane-strain compression geometry showing definition of specimen axes

conformation before quantitative results can be achieved[5].

All the techniques discussed so far can give $\langle P_2(\cos\alpha)\rangle$ and some also give $\langle P_4(\cos\alpha)\rangle$ and $\langle P_6(\cos\alpha)\rangle$[3]. However, none of them can give the complete orientation distribution function.

For crystalline materials, the most satisfactory method of measuring crystallite orientation is by using X-ray diffraction[6,7], since this gives a complete orientation distribution function rather than just the moments of the distribution[8]. Hence, it is very tempting to try using diffraction to measure orientation in non-crystalline polymers. However, in the 30 years since the anisotropic WAXS from plastically deformed glassy polymers was first investigated[9,10], there have only been a few rather unsuccessful attempts at measuring the orientation by this means[11-14].

The simplest measures of orientation are the azimuthal breadths of the diffuse haloes[6]. However, these are not very precise since increasing orientation could increase the peak-to-valley height of the azimuthal profile without reducing the breadth. A more accurate measure is obtained by calculating $\langle\cos^2\alpha\rangle$ but this has a number of difficulties for non-crystalline polymers.

To illustrate these problems, we first consider the X-ray determination of orientation in crystalline polymers. Although pole figures can be prepared, such detail is often unnecessary and it is sufficient to calculate $\langle\cos^2\alpha\rangle$ where α is the angle between the molecular axis (usually the *c*-axis of the crystals) and the specimen axis. Wilchinsky[8] has shown how $\langle\cos^2\alpha\rangle$ can be calculated for all crystal systems, but up to five reflections may be needed. However, for the common case of randomness about the molecular axis, the value of $\langle\cos^2\alpha\rangle$ can be calculated from a single, arbitrary reflection. Hence the strongest reflection is generally used; this is often equatorial (*hk*0).

Reflections from crystalline polymers are sharp enough for the required one to be easily separable from its neighbours, and for the background scattering to be substracted. The resulting azimuthal profile is then directly related to the distribution of molecular axes.

For non-crystalline polymers, the scattering is much more diffuse, making the separation from neighbouring haloes and the subtraction of the background more difficult. Moreover, the diffuseness implies that the tangential broadening is not only due to disorientation but also has an intrinsic component that would be present even in perfectly oriented polymer. Wilchinsky[12] and Ruland[14,15] have considered both these sources of error but have not developed a general approach to the problem.

The only compensation with non-crystalline polymers is that randomness about the segment axis almost certainly occurs, meaning that only one diffuse halo need be considered. For most polymers, the strongest halo orients towards the equator, which has the advantage that (particularly for long, straight segments) the equatorial scattering has less intrinsic azimuthal broadening than does the meridional scattering. However, for short or curved segments, the relationship between the equatorial scattering and the segmental orientation is less well defined.

All previous attempts at measuring orientation in non-crystalline polymers have used equatorial scattering. The most successful of these has been Wilchinsky's measurement of orientation in the amorphous component of drawn polyethylene[12] but others have worked on silicone rubber[16], atactic polystyrene[13,17] and nylons[14].

In this work, we have measured the segmental orientation in poly(methyl methacrylate) (PMMA) using a diffuse halo which intensifies towards the extension direction (thus, it is meridional rather than equatorial) and, therefore, comes from scattering within the chains rather than between chains. We compare this measure of orientation with that from birefringence for specimens which have been deformed either elastically or plastically.

EXPERIMENTAL

Specimens were cut from 3 mm thick commercial PMMA sheet (ICI Perspex) and their edges polished first with dry abrasive paper and then with Brasso metal polish*. They were annealed to remove all residual birefringence.

The specimens were then plastically deformed in plane-strain compression (*Figure* 1) using a rig with heated dies lubricated with Molyslip[18]. The advantages of using plane-strain compression[19] are that large amounts of plastic deformation can be achieved, and that the development of orientation during deformation can be monitored by measuring the birefringence (Δn_{zx}) using a plane polariscope[20]. Once the required deformation was reached, the specimen was unloaded (where necessary), cooled underload to below 80°C, then removed from the rig (i.e. air cooled). It was allowed to equilibrate at room temperature for at least 100 h before measurement. The residual birefringence (Δn_{zy} and Δn_{zx}) was measured using a six-order Berek compensator[21] in a polarizing microscope.

The disadvantages of using plane-strain compression are that it produces a biaxial orientation distribution and that the deformation is non-uniform throughout the specimen. The second of these was averted by making all measurements at the centre of the *yz* face of the specimens. The effects of biaxial orientation will be discussed later.

Wide angle X-ray scattering was measured using a symmetrical transmission diffractometer fitted with an Eulerian cradle to rotate each specimen about its *x*-axis. The scattering vector always lies in the *yz*-plane[22]. Copper $K\alpha$ radiation was used with a doubly-bent LiF

* The use of Silvo metal polish leads to premature fracture, presumably due to environmental degradation of the surfaces induced by the polish suspension medium.

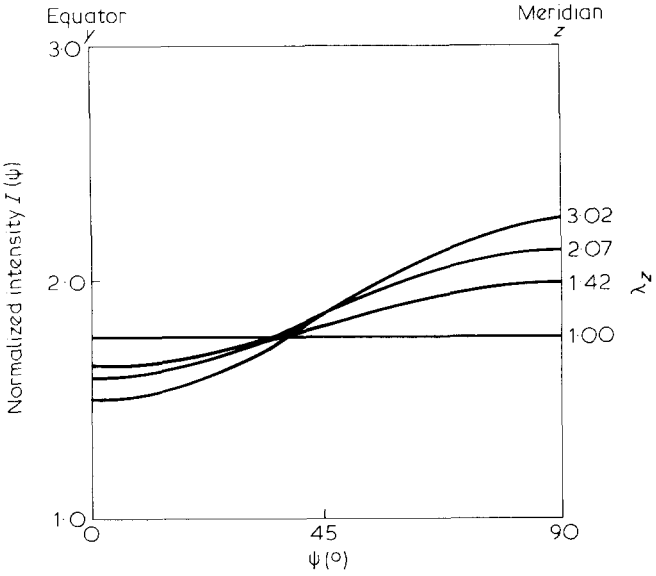

Figure 2 Azimuthal intensity profiles for 30° 2θ halo of PMMA specimens deformed in plane-strain compression at 100°C to different extension ratios

monochromator[23] in the direct beam to increase the incident intensity. The beam was limited to a 6 mm diameter circle on the centre of the yz face of each specimen.

The diffuse halo at $2\theta = 30^\circ$ ($s = 2.1\,\text{Å}^{-1}$ where $s = (4\pi \sin\theta/\lambda)$ was used to measure the segmental orientation. This halo has been shown to be intramolecular[24] (corresponding to spacings between sidegroups) and concentrates towards the meridian in plastically deformed specimens. Azimuthal profiles of this halo for specimens of different extension ratios are shown in *Figure* 2. All intensities were normalized to that at $2\theta = 38^\circ$ to allow for variations in specimen thickness. The intensity at 38° is unaffected by orientation (i.e. the azimuthal profile remains flat).

The X-ray examination of elastically strained material used the same diffractometer set-up, except that the specimens (1 mm thick) were mounted in a jig designed to maintain uniaxial tension.

Measurement of orientation parameters by WAXS

Comparison with birefringence. There are basic differences between the orientation parameters measured using birefringence and those measured using WAXS. These differences become more apparent when the specimens do not have cylindrical symmetry, plane-strain compression specimens, for example. The differences arise from the fact that, in a WAXS experiment, the specimen is rotated so that the scattering vector stays in a plane and, hence, the scattering only samples a cross-section of the orientation distribution function. However, molecules at all angles contribute to the birefringence.

For specimens with cylindrical symmetry, a section containing the unique axis is sufficient to define the distribution completely and, hence, WAXS and birefringence can give equivalent measurements. For specimens of lower symmetry, the measurements are no longer equivalent, although they are likely to remain approximately proportional.

To illustrate these effects, we have calculated the dependence of the orientation parameters on extension ratio assuming that deformation occurs by the pseudoaffine mechanism[3]. Below 60°C, the deformation of PMMA is most readily represented by this mechanism.

The orientation distribution function for a general pseudoaffine deformation has been given by Sasaguri, Hoshino and Stein[25]:

$$D(\alpha,\beta) = \frac{(\lambda_x\lambda_y\lambda_z)^2}{2\pi[\lambda_x^2\lambda_y^2\cos^2\alpha + \lambda_z^2\sin^2\alpha(\lambda_y^2\cos^2\beta + \lambda_x^2\sin^2\beta)]^{3/2}}$$

where α,β are the colatitude and longitude defined in *Figure* 3, λ_i is the extension ratio along the ith axis, and

$$\int_0^{2\pi}\int_0^{\pi/2} D(\alpha,\beta)\sin\alpha\,d\alpha\,d\beta = 1$$

For uniaxial deformation, at constant volume, $\lambda_x = \lambda_y = \lambda_z^{-1/2}$ so that this reduces to[26]:

$$D(\alpha) = \frac{\lambda_z^3}{2\pi(\cos^2\alpha + \lambda_z^3\sin^2\alpha)^{3/2}} \quad (1)$$

whereas, for plane-strain compression, $\lambda_x = 1/\lambda_z$ and $\lambda_y = 1$ giving:

$$D(\alpha,\beta) = \frac{\lambda_z^3}{2\pi[\cos^2\alpha + \lambda_z^2\sin^2\alpha(\lambda_z^2\cos^2\beta + \sin^2\beta)]^{3/2}} \quad (2)$$

We can use this expression to calculate the various averages needed for the orientation parameters.

For segments which are randomly distributed about their axes, the birefringence of a specimen with any distribution of orientations is given by:

$$\Delta n = n_z - n_y = \Delta n_{max}[\langle\cos^2\varphi_z\rangle - \langle\cos^2\varphi_y\rangle]$$

where φ_i is the angle between the segment axis and the ith specimen axis. This can be rewritten using

$$\cos\varphi_y = \sin\alpha\sin\beta$$

and

$$\cos\varphi_z = \cos\alpha$$

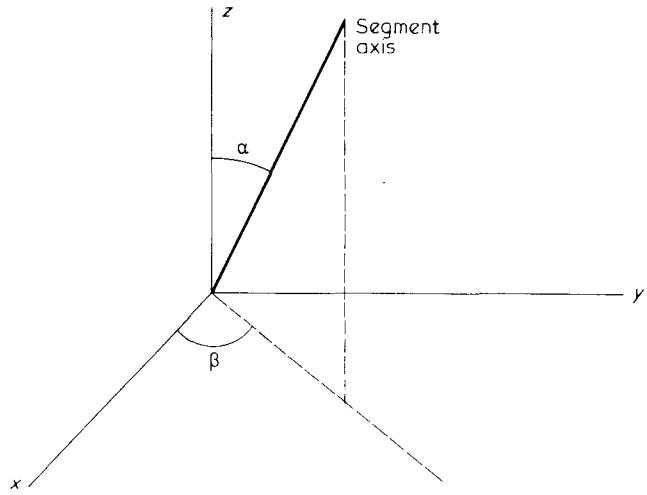

Figure 3 Polar coordinates defining direction of axis of chain segment relative to specimen axes

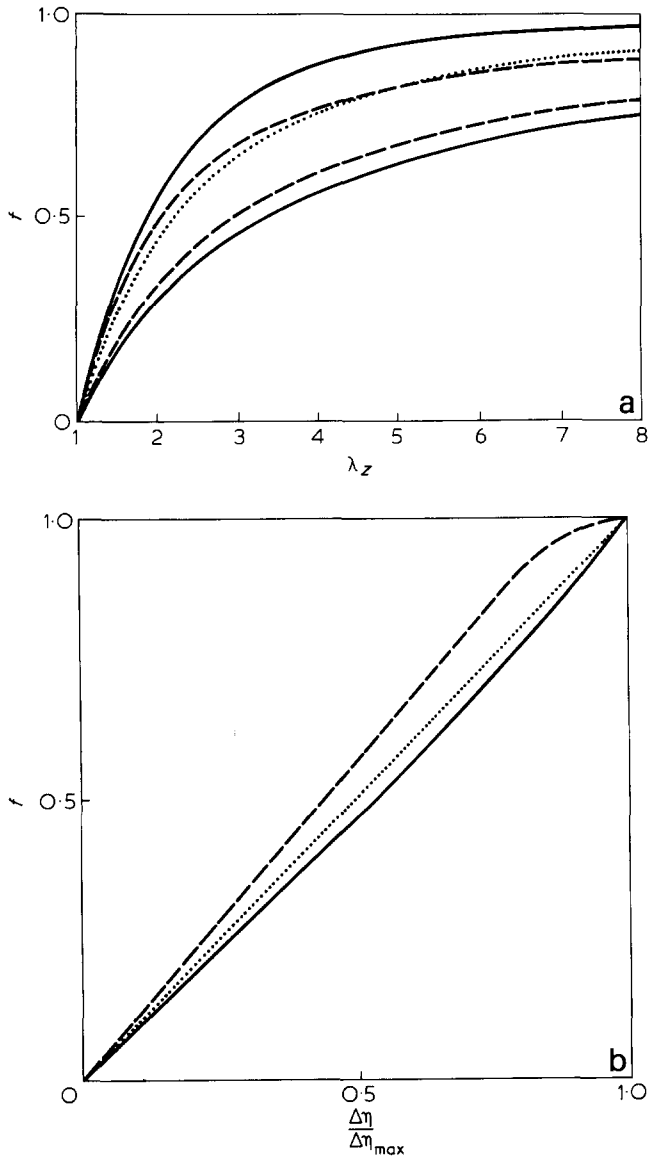

Figure 4 Comparison of X-ray orientation parameter (f) and birefringence ($\Delta n/\Delta n_{max}$) for uniaxial deformation and plane-strain compression. Pseudoaffine deformation assumed in both cases
(a) Plotted against extension ratio, λ_z
—— f } Plane-strain
– – – $\Delta n/\Delta n_{max}$ } compression
... f and $\Delta n/\Delta n_{max}$ Uniaxial
(b) f plotted against $\Delta n/\Delta n_{max}$
—— zy plane } Plane-strain
– – zx plane } compression
.... Uniaxial.

as $$\Delta n_{zy} = \Delta n_{max}[\langle \cos^2 \alpha \rangle - \langle \sin^2 \alpha \sin^2 \beta \rangle]$$

The necessary averages are calculated by numerical integration over all possible orientations.

In contrast, we can define an X-ray orientation parameter in the zy plane by:

$$f_{zy} = \frac{1}{2}[3\langle \cos^2 \alpha \rangle_{zy} - 1]$$

where the average $\langle\ \rangle_{zy}$ is calculated for segments lying in the zy plane only (i.e. $\beta = 90°$ or 270°). For plane-strain compression, the two orientation parameters

$$(\Delta n_{zy}/\Delta n_{max} \text{ and } f_{zy})$$

are no longer exactly equal; however, as shown in *Figure* 4, they are very nearly so, at least for pseudoaffine deformation.

The above treatment is strictly applicable only to crystallite orientation rather than to segmental orientation in a non-crystalline polymer. The differences will be discussed in the next section.

Intrinsic azimuthal width. The scattering from even a perfectly aligned, though non-crystalline, polymer would give diffuse spots with dimensions corresponding to the degree of order parallel and perpendicular to the chains[27]. In particular, even for a long straight chain, the meridional scattering will be spread along layer lines creating an intrinsic azimuthal width which will broaden the observed profile and reudce the value of the orientation parameter obtained.

The observed azimuthal profile is given by a form of convolution of the orientation distribution with the intrinsic profile[28]:

$$I(\psi) = \int_0^{\pi/2} \sin \alpha \int_0^{2\pi} D(\alpha,\beta) I_0(\gamma)\, d\beta\, d\alpha$$

where I_0 is the intrinsic profile and γ is the angle measured from the segment axis, given by: $\cos \gamma = \cos \alpha \sin \psi + \sin \alpha \cos \psi \sin \beta$.
For uniaxial symmetry, this simplifies to

$$I(\psi) = \int_0^{\pi/2} D(\alpha) \sin \alpha \int_0^{2\pi} I_0(\gamma)\, d\beta\, d\alpha$$

Expansion of I, I_0 and D in a series of Legendre polynomials shows that any orientation parameter $\langle P_{2n} \rangle$ derived from I is given by the product of the orientation parameters for I_0 and D (e.g. equation (31) of ref. 27). Hence, the ratio of observed and 'true' orientation parameters is constant for a given intrinsic width. This ratio is shown in *Figure* 5 for an intrinsic profile of the form:

$$I_0(\gamma) = \frac{1}{1 + (\gamma/\delta)^4} \qquad 0 \leqslant \gamma \leqslant \frac{\pi}{2}$$

which has roughly the shape expected, with a flat maximum at $\gamma = 0$. Intrinsic profiles of different widths are given by varying δ, the half width.

The intrinsic width for PMMA is, of course, unknown. Calculations of scattering from model single chains[29] would suggest a half-width of ~20°, whereas extrapolation of the measured half-widths to $1/\lambda = 0$ (*Figure* 6) would give 40° or more. Hence, the measured values of f are likely to be in the range of 60–80% of the 'true' values. Therefore, we have applied a correction factor to all the experimental values of f in this work:

$$f^{corr} = 1.4f \qquad (3)$$

Similar calculations by Ruland and Wiegand[14] have

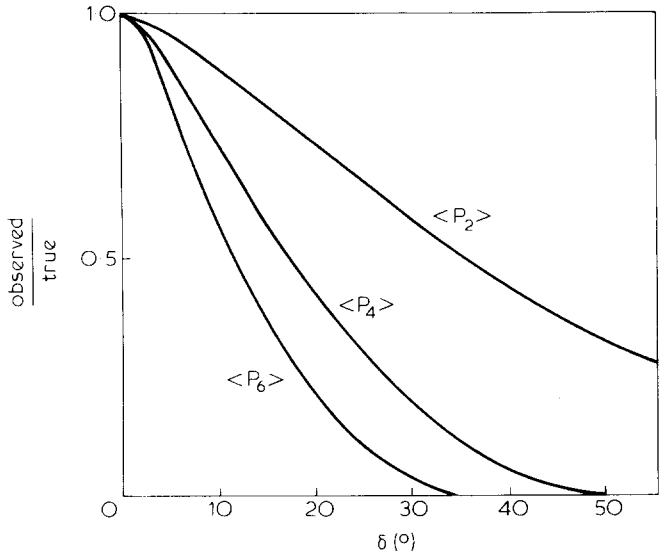

Figure 5 Effect of intrinsic azimuthal width on observed orientation parameters. Ratio of observed to 'true' orientation parameters as a function of half-width, δ, of the intrinsic azimuthal profile

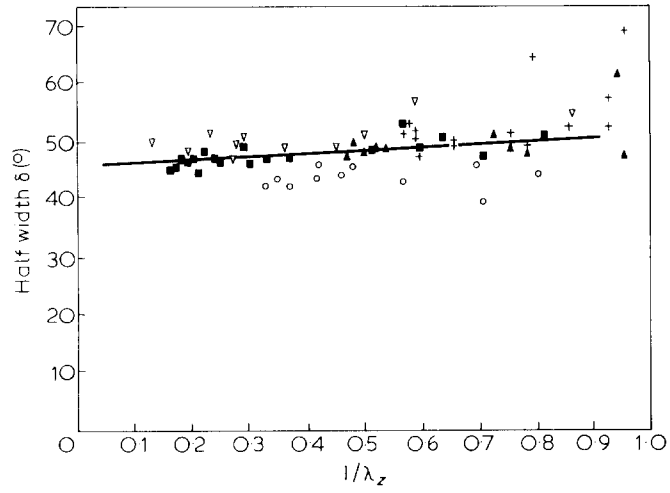

Figure 6 Extrapolation of observed azimuthal half-widths to infinite extension ratio. Specimens of PMMA deformed in plane-strain compression at various temperatures (+20°, ▲ 60°, ○ 100°, ■ 125°, △ 150° C)

$$\delta = \frac{\int_0^{\pi/2} [I(\psi) - I(0)]\, d\psi}{I(\pi/2) - I(0)}$$

shown that the error in f is $\sim 10\%$ for f less than 0.2 with an intrinsic half-width of $\sim 10°$.

Values of $\langle P_4(\cos\alpha)\rangle$ and $\langle P_6(\cos\alpha)\rangle$ are much more sensitive to the intrinsic width (see *Figure* 5) and, although they are useful measures of the orientation distribution, it is unreasonable to expect this WAXS method to give reliable indication of their values.

Background correction. The total scattered intensity at $2\theta = 30°$ (CuKα) not only consists of the required intramolecular scattering but also includes the tails of diffuse haloes at $2\theta = 13°$ and 42°, as well as elastic and inelastic scattering which are insensitive to orientation. Unless these other components are removed, the calculated orientation parameters will be too low, especially for the higher orientations.

Although the tails of the other haloes may have an azimuthal dependence, we have assumed that an adequate background correction can be made by subtracting a constant intensity (I_B) from the azimuthal scans. We have tried a number of ways of estimating this background intensity.

Firstly, as shown in *Figure* 2, the equatorial intensity of the halo decreases as the meridional intensity increases. Hence, we can assume that, particularly for uniaxial deformation, at infinite extension the intensity on the equator at $2\theta = 30°$ (I_{eq}) would have reached the background level. Therefore, we can estimate I_B by extrapolating I_{eq} to $\lambda_z = \infty$. For uniaxial deformation by the pseudoaffine mechanism, equation (1) shows that plotting I_{eq} against $\lambda_z^{-3/2}$ should give a straight line. *Figure* 7 shows a plot for specimens deformed in uniaxial tension at 100°C. Extrapolation to $\lambda_z^{-3/2} = 0$ (i.e. infinite extension) gives $I_B = 1.3$.

A similar plot for specimens deformed in plane-strain compression is shown in *Figure* 8. However, equation (2) predicts that I_{eq} should be independent of λ_z since segments exactly parallel to the y-axis should remain parallel after

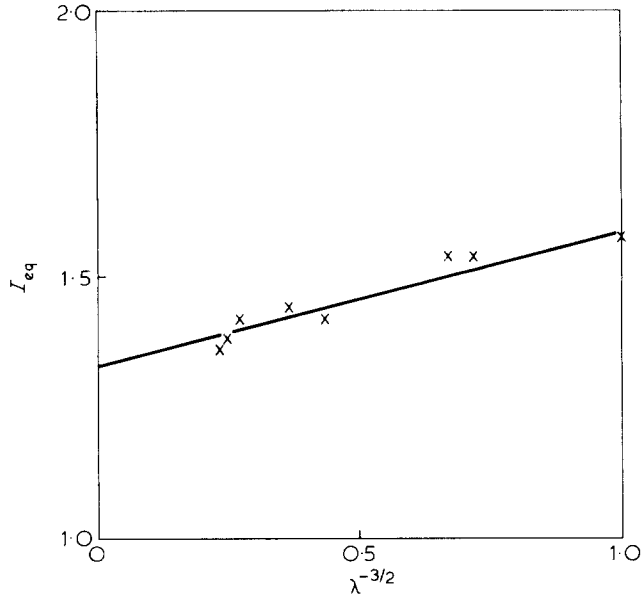

Figure 7 Extrapolation of equatorial intensity at 30° 2θ to infinite extension ratio for PMMA specimens deformed in uniaxial extension at 100° C

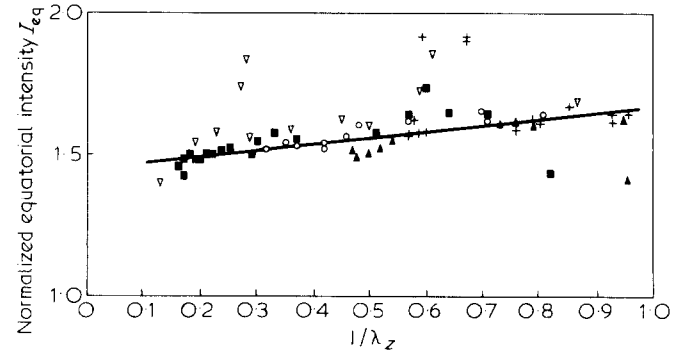

Figure 8 Variation of I_{eq} with extension ratio for plane-strain compression specimens deformed at various temperatures (+ 20°, ▲ 60°, ○ 100°, ■ 125°, △ 150° C)

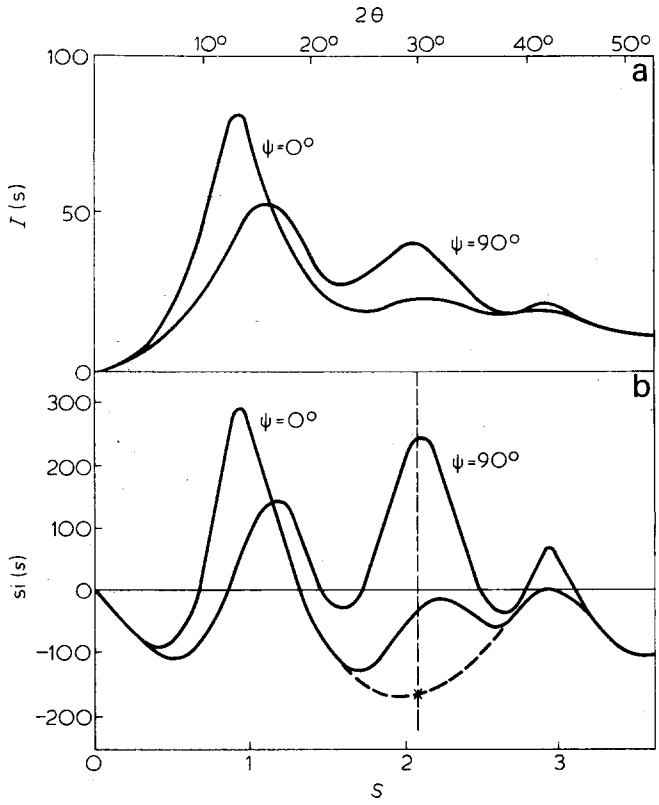

Figure 9 (a) Equatorial and meridional scans and (b) *s*-weighted reduced intensity functions si (s) for a specimen deformed in plane-strain compression at 100°C. $\lambda_z \approx 3$ si (s) = $s[kI(s) - \Sigma f^2(s)]$ (See ref. 29)

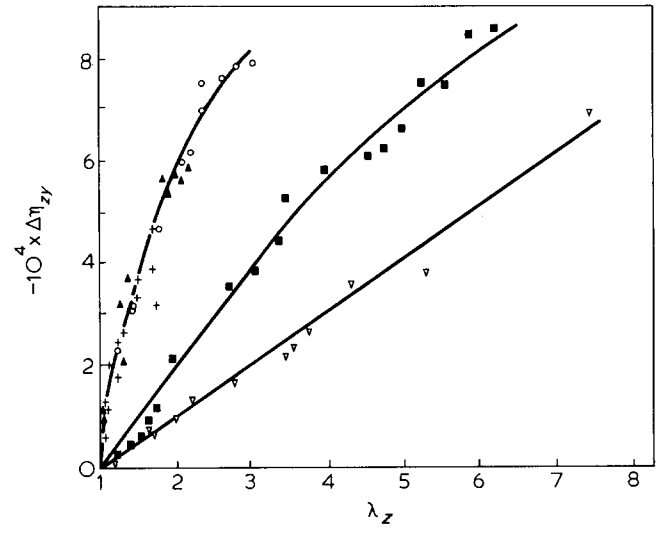

Figure 10 Residual birefringence (measured at room temperature) as a function of extension ratio for plane-strain compression specimens deformed at various temperatures (+ 20°, ▲ 60°, ○ 100°, ■ 125°, △ 150°)

deformation. The observed decrease in I_{eq} with increasing λ_z is due to the intrinsic azimuthal width. Because of the smearing, segments that are not exactly parallel to the *y*-axis also contribute to I_{eq} but these segments align towards the *z*-axis as the specimen deforms, causing a reduction in I_{eq}. In view of this uncertainty, we have not extrapolated the plane-strain data.

Observed departures from pure plane-strain compression (bowing of the *xz* faces of specimens at large deformations) should lead to I_{eq} *increasing* with λ_z.

The second method is to attempt to sketch in a background with reference to scattering at neighbouring 2θ values. This is similar to the method used for semi-crystalline polymers.

Figure 9 shows equatorial and meridional scans for a highly oriented specimen together with the corresponding reduced intensity functions, *si* (s)[29]. The background sketched for the equatorial *si* (s) gives a value for I_B of ~ 1.0.

From the two methods, it seems that I_B lies in the range 1.0–1.3. We have adopted a value of 1.1 in the results that follow.

RESULTS AND DISCUSSION

Plastic deformation in plane-strain compression

Figure 10 shows the residual birefringence Δn_{zy} as a function of λ_z for deformation at temperatures between 20° and 150°C, whereas *Figure* 11 shows the values of f_{zy}^{corr} derived from X-ray measurements on the same specimens. It can be seen that the dependence is very similar. In *Figure* 12, Δn_{zy} is plotted against f_{zy}^{corr}. Within experimental error, the points are scattered about a single straight line indicating a proportionality constant independent of deformation temperature. This shows that f_{zy} calculated from X-ray scattering is as good a measure of orientation as is birefringence. The results can be taken to imply that Δn_{max} is not sensitive to deformation temperature (i.e. that specimens deformed at different temperature have similar molecular conformations).

Figures 10 and 11 show the much slower development of orientation with deformation of the rubber than in the glass (for PMMA, $T_g \approx 110$°C). This is a well-known phenomenon, similar results having been found for

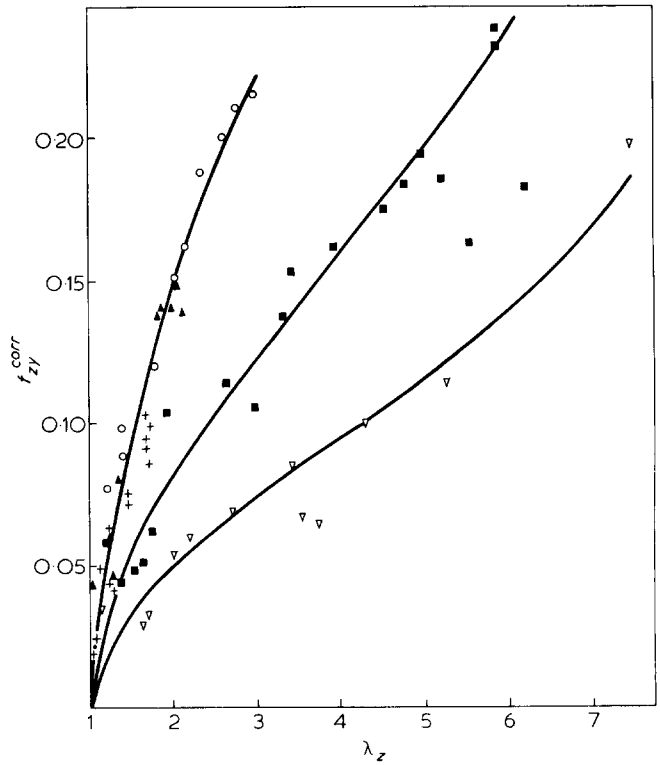

Figure 11 WAXS orientation parameter as a function of extension ratio for the same specimens as in *Figure 10*

PMMA and PET using birefringence[18,30,31]. In *Figure* 13 we plot the observed f_{zy}^{corr} against that expected from the pseudoaffine mechanism at the same extension ratio. The linear relationship at low temperatures supports the pseudoaffine mechanism. However, the fact that the gradient is less than unity needs explanation. It is possible that the orientation process does not involve all the segments or, alternatively, that the segments are associated into anisotropic regions in which there is a limited orientational correlation, and it is the alignment of the regions which contribute to the observed orientation.

Plastic deformation in uniaxial extension

The Table shows measurements made on specimens of commercial PMMA which had been drawn at temperatures between 95 and 140°C. The specimens were lent by Professor Ward of the University of Leeds and are some of those originally prepared by the Department of Polymer and Fibre Science, UMIST. They have been studied by Kashiwagi, Folkes and Ward[5] using broad-line n.m.r., and Purvis and Bower[32] have examined similar specimens using polarized Raman. The values of f^{corr} which we have calculated from WAXS measurements on the same specimens are in reasonably good agreement with those measured with n.m.r.[5].

The n.m.r. measurement of orientation needed to assume a particular conformation for the polymer chain (taken to be an isotactic 5/1 helix[5]), whereas our only assumption for the X-ray measurement was to use the same corrections as for our own specimens.

Elastic deformation in uniaxial tension

For elastically strained specimens, there is an apparent orientation of the first (intermolecular) halo. But this is due to elliptical distortion of the halo rather than a redistribution of intensity as a function of azimuthal angle. This is discussed in a separate publication[33].

Figure 14 shows f and Δn plotted against λ_z for tensile specimens deformed elastically at room temperature. It can be seen that the amount of birefringence is comparable with that produced in plastic deformation but that the WAXS orientation parameter is not significantly different from zero even at the highest elastic strains obtainable before fracture. This shows that the photoelastic effect in PMMA is not due to alignment of the polymer chains. We have discussed elsewhere[34] a possible explanation of the birefringence produced by elastic strain.

Values of $\langle P_4(\cos\alpha)\rangle$

Experimental values of $\langle P_4(\cos\alpha)\rangle$ for the plastically deformed specimens were scattered within the range -0.008 to $+0.01$. If we multiply these by a correction factor of 3 (see equation (3) and *Figure* 5), the maximum $\langle P_4(\cos\alpha)\rangle$ would be about 10% of $\langle P_2(\cos\alpha)\rangle$, this would be in broad agreement with measurements made by n.m.r.[5] (*Table* 1).

GENERAL DISCUSSION OF TECHNIQUE

Advantages

There are two distinct advantages of the X-ray method of orientation measurement.

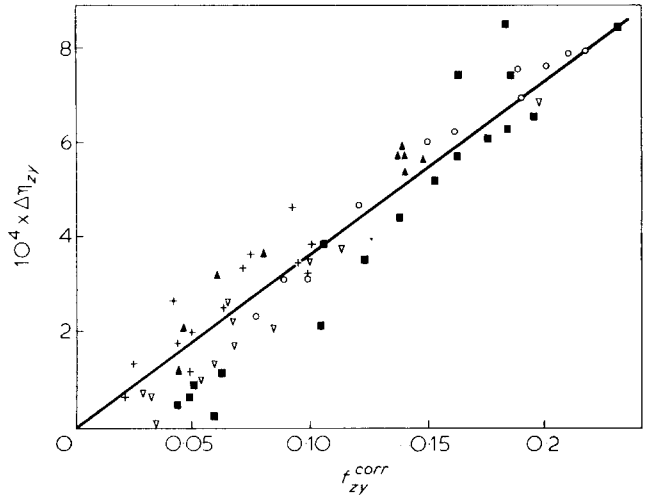

Figure 12 Comparison of WAXS orientation parameter with birefringence for the same specimens as in *Figures 10* and *11*. For plane-strain compression, the points should lie on a slight curve, at least for the pseudoaffine model. (See *Figure 4b*).

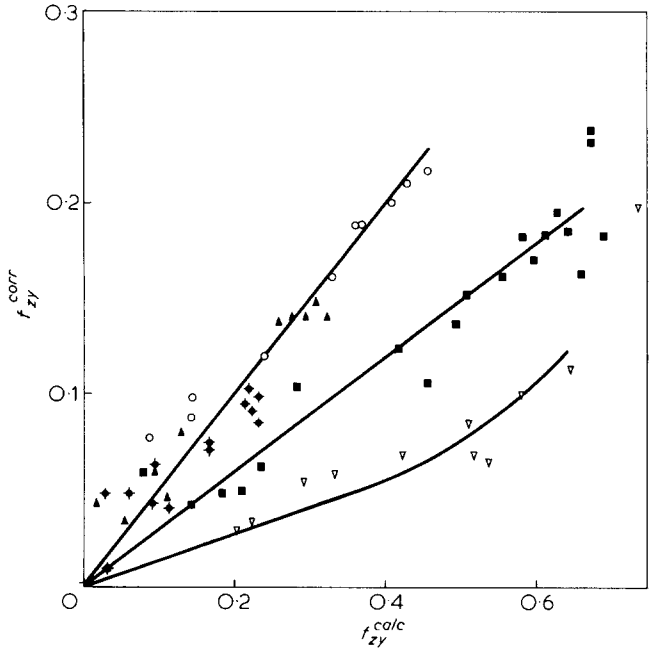

Figure 13 Comparison of the WAXS orientation parameter with that predicted by the pseudoaffine deformation scheme for plane-strain compression specimens at various temperatures (+ 20°, ▲ 60°, ○ 100°, ■ 125°, △ 150°C)

Table 1 Comparison of orientation parameters measured by different techniques

Specimen	Deformation temperature (°C)	Birefringence $10^4 \times \Delta n$	WAXS f^{corr}	n.m.r.[5] $\langle P_2(\cos\alpha)\rangle$	n.m.r.[5] $\langle P_4(\cos\alpha)\rangle$
AN	95	−13.2	0.29	0.307	0.049
BF	123	− 5.7	0.11	0.167	0.027
AE	140	− 3.5	0.08	0.055	−0.031

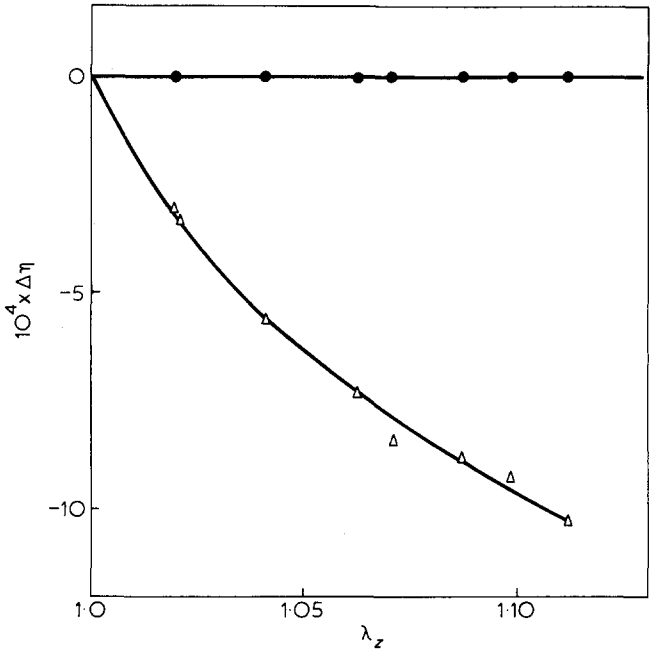

Figure 14 WAXS orientation parameter (●) and strain birefringence (△) measured on tensile specimens during elastic strain. Any WAXS orientation present is less than the minimum observable amount, and the data points have been assigned zero values

Firstly, the X-ray scattering comes from interference along the chains, hence, increased scattering in a given direction is due to alignment of chains in that direction rather than to rotation of sidegroups or to other conformational changes. This is in contrast to methods such as birefringence in which Δn_{max} might change with deformation temperature or infrared dichroism in which the angle between the transition vector and the chain axis might alter.

Secondly, no specific model of the chain conformation is needed. n.m.r. in particular requires the assumption of a definite conformation for the chain segments.

Disadvantages

The two main disadvantages of the X-ray method have been discussed in an earlier section.

Firstly, the estimation of the necessary background correction is difficult. This leads to error in the estimated orientation parameter, although it is still in an approximately constant ratio to the true value.

Secondly, the intrinsic component of the azimuthal width means that the initially calculated orientation parameter, $f(=\langle P_2(\cos\alpha)\rangle)$ will always be too low, although an approximate correction factor can be estimated. However, the higher moments $\langle P_4(\cos\alpha)\rangle$ and $\langle P_6(\cos\alpha)\rangle$ are much more strongly affected, meaning that no reliable measure of them can be made.

ACKNOWLEDGEMENTS

We are grateful to Geoffrey Mitchell for discussions and support throughout this work, to Professor I. M. Ward and Dr. R. A. Duckett of the University of Leeds for their interest and the loan of specimens, and to Professor R. W. K. Honeycombe for the provision of facilities. Financial support was provided by the Science Research Council.

REFERENCES

1 Stein, R. S. and Read, B. E. *Appl. Polym. Symposia* 1969, **8**, 255
2 Read, B. E. in 'Structure and Properties of Oriented Polymers' (Ed. I. M. Ward) Applied Science, London, 1975, Ch. 4
3 Ward, I. M. *J. Polym. Sci. (Polym. Symp.)* 1977, **58**, 1
4 Bower, D. I. in 'Structure and Properties of Oriented Polymers' (Ed. I. M. Ward) Applied Science, London, 1975, Ch. 5
5 Kashiwagi, M., Folkes, M. J. and Ward, I. M. *Polymer*, 1971, **12**, 697
6 Alexander, L. E. 'X-ray Diffraction Methods in Polymer Science' Wiley, New York, 1969, Ch. 4, p 262
7 Kakudo, M. and Kasai, N. 'X-ray Diffraction by Polymers', Elsevier, Amsterdam, 1972, Ch. 10
8 Wilchinsky, Z. W. *Advantages in X-ray Analysis* 1963, **6**, 231
9 Robinson, H. A., Ruggy, R. and Slantz, E. *J. Appl. Phys.* 1944, **15**, 343
10 Krimm, S. and Tobolsky, A. V. *Textile Res. J.* 1951, **21**, 805
11 Alexander, L. E., Ohlberg, S. M. and Taylor, G. R. *J. Appl. Phys.* 1955, **26**, 1068
12 Wilchinsky, Z. W. *J. Polym. Sci.* (A-2) 1968, **6**, 281
13 May, M., Walther, C. and Rufke, B. *Plaste und Kautschuk* 1975, **22**, 551
14 Ruland, W. and Wiegand, W. *J. Polym. Sci. (Polym. Symp.)* 1977, **58**, 43
15 Ruland, W. *J. Appl. Phys.* 1967, **38**, 3585
16 Ohlberg, S. M., Alexander, L. E. and Warrick, E. L. *J. Polym. Sci.* 1958, **27**, 1
17 Tanabe, Y. and Kanetsuna, H. *J. Appl. Polym. Sci.* 1978, **22**, 1619
18 Raha, S. and Bowden, P. B. *Polymer*, 1972, **13**, 174
19 Williams, J. G. and Ford, H. *J. Mech. Eng. Sci.* 1964, **6**, 405
20 Holister, G. S. 'Experimental Stress Analysis' Cambridge, 1967, p 146
21 Hartshorne, N. H. and Stuart, A. 'Crystals and the Polarising Microscope', 4th edition, Arnold, London, 1970, p 298
22 Lovel, R. and Windle, A. H. *Polymer* 1976, **17**, 488
23 Schwartz, L. H., Morrison, L. A. and Cohen, J. B. *Advances in X-ray Analysis* 1964, **7**, 281
24 Colebrooke, A. and Windle, A. H. *J. Macromol. Sci. Phys.* 1976, **B12**, 373
25 Sasaguri, K., Hoshino, S. and Stein, R. S. *J. Appl. Phys.* 1964, **35**, 47
26 Arridge, R. G. C. 'Mechanics of Polymers', Clarendon Press, Oxford, 1975, p 170
27 Vainshtein, B. K. 'Diffraction of X-rays by Chain Molecules' Elsevier, Amsterdam, 1966, Ch. 7
28 Ruland, W. and Tompa, H. *Acta Crystallogr.* 1968, **A24**, 93
29 Lovell, R. and Windle A. H. *Polymer* 1980, **21**, in press
30 Kahar, N., Duckett, R. A. and Ward, I. M. *Polymer* 1978, **19**, 136
31 Allison, S. W. and Ward, I. M. *Br. J. Appl. Phys.* 1967, **18**, 1151
32 Purvis, J. and Bower, D. I. *Polymer* 1974, **15**, 645
33 Pick, M., Lovell, R. and Windle, A. H. *Nature* 1979, **281**, 658
34 Pick, M. and Lovell, R. *Polymer* 1979, **20**, 1448